行政院國家科學委員會專題研究計畫　期中進度報告

鐵-鋁-錳(鎳)-碳-(矽,鈦,鈮,釩)合金相變化(1/2)

計畫類別：個別型計畫
計畫編號：NSC91-2216-E-009-019-
執行期間：91年08月01日至92年07月31日
執行單位：國立交通大學材料科學與工程學系

計畫主持人：劉增豐

報告類型：精簡報告

處理方式：本計畫可公開查詢

中　華　民　國 92年5月30日

Phase transformations in an
Fe-8.8Al-30Mn-5Cr-1.2Si Alloy

J. W. Lee and T. F. Liu

Department of Materials Science and Engineering, National Chiao Tung University,
Hsinchu, Taiwan, Republic of China

(NSC91-2216-E-009-019)

Abstract

The microstructure of the Fe-8.8Al-30Mn-5Cr-1.2Si alloy have been investigated by means of transmission electron microscopy. In the as-quenched condition, the extremely fine $D0_3$ particles were formed within the ferrite(α) matrix during quenching by a continuous ordering transition. When the alloy was aged at temperatures ranging from 450°C to 950°C, the phase transformation sequence as the aging temperature increases was found to be $(\alpha+D0_3+\alpha\text{-Mn})\rightarrow(\alpha+D0_3+\beta\text{-Mn})\rightarrow(\alpha+\beta\text{-Mn})\rightarrow\alpha$, in which no evidence of B2 phase could be detected. This is quite different from that observed in the Fe-Al-Mn-Si alloy. In the present study, the coexistence of the $D0_3$ phases with coarse and extremely fine size has never been found by other workers in the Fe-Al-Mn-Cr-Si alloys before.

Keywords : ordered $D0_3$*, phase, continuous ordering transition, Fe-Al-Mn-Cr-Si alloy*

1. Introduction

For economic and strategic considerations, manganese and aluminum are used to substitute for nickel and chromium added to the conventional stainless steels. In order to further improve the corrosion resistance and high-temperature oxidation resistance, chromium or silicon has been added to the Fe-Al-Mn alloys[1-7]. Based on their studies, it can be generally concluded that the addition of a small amount of chromium or silicon can effectively improve these properties.

We first performed transmission electron microscopy (TEM) observations on the phase transformations of Fe-Al-Mn-Cr alloys[8-12]. In the as-quenched condition, no extremely fine $D0_3$ particles could be detected within the ferrite grains. When the as-quenched alloys were aged at temperatures ranging from 350 to 520℃ or above, both ordered $D0_3$-type and A12 α-Mn precipitates were formed within the ferrite matrix. As increasing aging temperature to 550℃ or above, the β-Mn precipitates were observed and identified[11]. The orientation relationship and axis/angle pair of rotation between the β-Mn precipitates and the ferrite matrix were determined to be $(001)_{\alpha}//(012)_{\beta\text{-Mn}}$, $(010)_{\alpha}//(02\bar{1})_{\beta\text{-Mn}}$, $(100)_{\alpha}//(100)_{\beta\text{-Mn}}$ and $[100]/26^{\circ}$, respectively [12]. The phase transformations in an Fe-9.0Al-29.5Mn-1.2Si alloy were also investigated by the present workers[14]. Based on our previous study, it is found that the extremely fine $D0_3$ particles were formed within the ferrite matrix during quenching by a continuous ordering transition. After being aged at temperatures ranging from 550 to 950℃, a complex phase transition $(\alpha+D0_3+\text{L-phase})\rightarrow(\alpha+D0_3+\beta\text{-Mn})\rightarrow(B2+D0_3+\beta\text{-Mn})\rightarrow(B2+\beta\text{-Mn})\rightarrow(\alpha+\beta\text{-Mn})\rightarrow(\alpha+\gamma)\rightarrow\alpha$ has occurred within the ferrite grain. However, up to date, information concering the microstructural development of the Fe-Al-Mn-Cr-Si alloys are deficient. Therefore, the purpose of this work is an attempt to examine the phase transformations in an Fe-8.8Al-30Mn-5.0Cr-1.2Si alloy.

2. Experimental procedure

The alloy of composition Fe-8.8Al-30Mn-5.0Cr-1.2Si was prepared in a vacuum induction furnace by using 99.5% iron, 99.7% aluminum, 99.9% manganese, 99.5% chromium and ferrosilicon. After being homogenized at 1200℃ for 12 hours under a controlled protective argon atmosphere, the ingots was hot-forged and then cold-rolled to a final thickness of 2.0mm. The sheet was subsequently solution heat-treated at 1050℃ for 1 hour and rapidly quenched into room-temperature water. Aging processes were carefully performed at temperatures ranging from 450 to 950℃ for various times in a muffle furnace under a controlled protective argon atmosphere and then quenched.

Transmission electron microscopy specimens were prepared by means of a double-jet electropolisher with an electrolyte of 60% acetic acid, 30% ethanol, and 10% perchloric acid. Electron microscopy was performed on a JEOL-2000FX scanning transmission electron microscope operating at 200kv. This microscope was equipped with a Link ISIS300 energy-dispersive X-ray spectrometer (EDS) for chemical analysis. Quantitative analyses of elemental concentrations for Fe, Al, Mn, Cr and Si were made with the aid of a Cliff-Lorimer Ratio Thin Section method.

3. Results and discussion

Optical microscopy examination was taken to exhibit the microstructure of the alloy solution heat-treated at 1050oC for 1 hour and the quenched. It reveals a single-phase microstructure. Fig 1(a) is a bright-field (BF) electron micrograph of the as-quenched alloy. Figures 1(b) and (c) are two selected-area diffraction patterns

(SADPs) taken from the matrix in Figure 1(a). The zone axis are [001] and $[01\bar{1}]$, respectively. It is seen that in addition to the reflection spots corresponding to the disordered ferrite phase (α) the diffraction patterns also consist of small superlattice spots of 111, 200 etc. caused by the presence of precipitates. Based on the diffraction patterns, it is confirmed that the precipitates have an ordered fcc structure which belong to the $D0_3$-type. The orientation relationship between the ferrite phase and the ordered $D0_3$ phase was determined to be $(002)_{D03}$// $(002)_{\alpha}$ and $[110]_{D03}$// $[110]_{\alpha}$. The 111 $D0_3$ and 200 $D0_3$ (or equivalently 100 B2) dark-field (DF) electron micrograph are shown in Figures 1(d) and (e), respectively, revealing that the 111 and 200 DF image are morphologically identical. Since the 200 reflection spot comes from both the B2 and $D0_3$ phases, while the 111 reflection spot comes only from the $D0_3$ phase, the extremely fine bright particles presented in Figures 1(d) and (e) are considered to be the $D0_3$ phase, and not B2 phase. It is reasonable to suppose that the extremely fine $D0_3$ particles were formed within ferrite matrix during quenching process from 1050^{o}C to room temperature by a continuous ordering transition; otherwise the $D0_3$ particles would grew rapidly at a high temperature of 1050^{o}C. On the basis of the above observations, it is concluded that the microstructure of the alloy in the as-quenched condition was the ferrite phase containing the extremely fine $D0_3$ particles. The extremely fine $D0_3$ particles were form during quenching by a continuous ordering transition. Additionally, it is worthy to note that no evidence of the small B2 domains with a/4<111> antiphase boundaries (APBs) could be detected using a 200 $D0_3$ reflection in the present study. The result of the absence of the a/4<111> APBs is quite different from that observed in our previous study in the Fe-9.0Al-29.5Mn-1.2Si alloy. Accordingly, the as-quenched microstructure of the present alloy was the ferrite phase containing the extremely fine $D0_3$ particles.

Figure 2(a) and (b) are the BF electron micrograph and SADP of the alloy after being aged at 450°C for 4 hours. It is seen in the 111 and 200 $D0_3$ DF electron micrograph, as shown in Figures 2(c) and (d), respectively, that the extremely fine $D0_3$ particles existing in the as-quenched alloy have grown slightly within the ferrite matrix during the early stage of isothermal aging at 450°C. Figure 3(a), a BF electron micrograph of the alloy aged at the same temperature for a long period of time, shows that the coarse precipitates were homogeneously formed within the matrix. As shown in Figure 3(b), an SADP taken from an area covering the coarsen precipitates and the surrounding matrix, indicates that in addition to the original $D0_3$ phase, another kind of precipitate corresponding to the rather faint diffraction spots could be detected. According to the camera length and the measurements of angles as well as the d-spacings of the rather faint diffraction spots, the crystal structure of the precipitates was determined to be a complex body-centered cubic with lattice parameter a=0.8889nm, which is consistent with that of the A12 α-Mn. Figures 3(c) and (d), 111 and 200 $D0_3$ DF electron micrographs, respectively, clearly illustrated that the coarse $D0_3$ particles were homogeneously formed within the ferrite matrix. Additionally as shown in Figure 3(e), a 011 α-Mn DF electron micrograph, exhibits the presence of a less amount of the fine α-Mn precipitates. Based on the above observations, it is concluded that the microstructure of the present alloy in the equilibrium stage at 450°C was a mixture of ($\alpha+D0_3+\alpha$-Mn) phases.

When the alloy was aged at 550°C for 24 hours and then quenched, the plate-like precipitates occurred within the matrix as shown in Figure 4(a). Figure 4(b) is an SADP taken from an area covering the plate-like precipitate and its surrounding matrix. Electron diffraction demonstrated that the plate-like precipitates were β-Mn and the orientation relationship between the β-Mn and the ferrite matrix is $(001)_{\alpha}//(012)_{\beta\text{-Mn}}$, $(010)_{\alpha}//(02\bar{1})_{\beta\text{-Mn}}$ and $(100)_{\alpha}//(100)_{\beta\text{-Mn}}$ [12]. Figures 4(c) and (d) are

111 and 200 DF electron micrographs, respectively, revealing that the well-grown $D0_3$ particles were densely formed within the ferrite matrix. It is noted the $D0_3$ particles surrounding the β-Mn precipitates are much larger than those away from the β-Mn phase. On the basis of the above observations, a $(\alpha + D0_3 + \alpha\text{-Mn}) \rightarrow (\alpha + D0_3 + \beta\text{-Mn})$ transition has occurred in the alloy at a temperature between 450 and 500℃.

A further increase in aging temperature up to 650℃, the β-Mn precipitate marked as B has grown considerable within the ferrite matrix, as shown in Figure 5(a). Figure 5(b), a 111 DF electron micrograph of the same area as Figure 5(a), exhibits the coexistence of both the coarse and extremely fine $D0_3$ particles. Since the size of the extremely fine $D0_3$ particles are comparable to that observed in the as-quenched alloy. It is thus suppose that the coarse $D0_3$ particles should be formed at the aging stage by a nucleation and growth mechanism; however, the extremely fine $D0_3$ particles should be formed during quenching from aging temperature by a continuous ordering transition. Furthermore, since the 200 DF electron micrograph is morphologically identical to 111 DF electron micrograph, as shown in Figure 5(c), no evidence of the B2 phase could be detected and the $D0_3$ phase was still preserved at 650℃ in the present alloy, which is different from that observed in our previous study in the Fe-9.0Al-29.5Mn-1.2Si alloy[14]. Accordingly, the microstructure of the present alloy aged at 650℃ and then quenched was a mixture of (α + β-Mn + coarse $D0_3$+ fine $D0_3$) phases, in which the fine $D0_3$ particles were formed during quenched by a continuous ordering transition.

Figure 6(a) is a BF electron micrograph of the alloy aged at 750℃ for 6 hours. The β-Mn precipitate marked as B in Figure 6(a) has grown rapidly and occupied the alloy with a considerable volume fraction, as shown in Figure 6(b). Figure 6(c) and (d) are 111 and 200 DF electron micrographs, respectively, demonstrating the existence of the extremely fine $D0_3$ particles within the ferrite matrix. Based on the same reason mentioned above, the stable microstructure of the present alloy aged at 750℃ was a mixture of ($\alpha+\beta$-Mn) phases. The extremely fine $D0_3$ particles were formed within the ferrite matrix during quenching by a continuous ordering transition. Transmission electron microscopy examinations revealed that the stable microstructure of the ($\alpha+\beta$-Mn) phases could be preserved up to a temperature between 900 and 950℃. When the alloy was aged at 950℃ and then quenched, only extremely fine $D0_3$ particles were formed within the ferrite, as shown in Figure 7, which is similar to that observed in the as-quenched alloy. This indicates that the microstructure of the present alloy aged at 950℃ or above should be the ferrite phase.

On the basis of the above observations, it is clear that when the present alloy was aged at temperatures ranging from 450 to 950^{o}C, the phase transformation sequence was found to be $(\alpha+D0_3+\alpha\text{-Mn})\rightarrow(\alpha+D0_3+\beta\text{-Mn})\rightarrow(\alpha+\beta\text{-Mn})\rightarrow\alpha$. The extremely fine $D0_3$ particles were formed within the α matrix during quenching from aging temperature at 650^{o}C or above. The results have never been found in the Fe-Al-Mn-Si alloys before. Compared to our previous study[14], the 111 DF election micrograph of the as-quenched Fe-9Al-29.5Mn-1.2Si alloy exhibited the presence of extremely fine $D0_3$ particles, which is similar to that of the present as-quenched alloy. It is likely to suggest that the as-quenched microstructures of both alloys are alike. Nevertheless, the DF electron micrography examination using a 200 reflection spot revealed that the small B2 domains with a/4<111> APBs were formed throughout the ferrite grain in the as-quenched Fe-9Al-29.5Mn-1.2Si alloy. It is thus that a $\alpha\rightarrow B2\rightarrow D0_3$ continuous ordering transition was occurred during quenching in the as-quenched Fe-9Al-29.5Mn-1.2Si alloy. In the present as-quenched alloy; on the contrary, since the 111 and 200 DF electron micrographs are morphologically identical, no evidence of the small B2 domains with a/4<111> APBs could be detected. For the reason of the absence of the a/4<111> APBs, instead of a $\alpha \rightarrow B2 \rightarrow D0_3$, a $\alpha \rightarrow D0_3$ continuous ordering transition should be occurred during quenching from quenching temperature in the present alloy. Moreover, the existence of B2 phase could be observed in the Fe-9Al-29.5Mn-1.2Si alloy present at 650 or 700^{o}C. In the present alloy; however, no evidence of B2 phase could be detected in the present alloy aged at temperature ranging from 450 to 950^{o}C. For comparison, in addition to contain 5wt% Cr, the chemical composition of the present alloy is similar to that of the Fe-9Al-29.5Mn-1.2Si alloy. Consequently, it is generally concluded that the addition of 5 wt% Cr to the Fe-9Al-29.5Mn-1.2Si alloy would not only change a continuous ordering transition from $\alpha \rightarrow B2 \rightarrow D0_3$ to $\alpha \rightarrow D0_3$, but also expand the $D0_3$ phase-field region.

When the alloy was aged at 550^{o}C, a high density of the well-grown $D0_3$ particles was present. It demonstrates that the well-grown $D0_3$ particles should be formed during aging stage by a nucleation and growth mechanism. However, compared Figure 4(c) whit 5(c), 111 $D0_3$ DF electron micrographs of the alloy aged at 550 and 650^{o}C, respectively, it is obvious that besides the coarse $D0_3$ particles, another $D0_3$ particles with extremely fine size formed within the remaining ferrite matrix during quenching from 650^{o}C by a ordering transition were observed in Figure 5(c). As increasing the aging temperature to 750^{o}C or above, only the extremely fine $D0_3$ particles were detected, but the coarse $D0_3$ particles were absent. The coexistence of the $D0_3$ particles with coarse and extremely fine size is a remarkable feature in the present study, which has never been observed by other workers in the Fe-Al-Mn-Cr-Si alloys before. In order to clarify this feature, an STEM-EDS study was undertaken. The average concentrations of the substitutional alloys elements were obtained from at least ten different EDS profiles of each phase. The results are summarized in Table I. It is clearly seen in Table I that the coarse $D0_3$ particles observed in the alloy aged at

550 or 650^{o}C are enriched in silicon. Therefore, after being aging at 550^{o}C, since the formation of a high density of the coarse $D0_3$ particles, the remaining ferrite matrix would contain less silicon. For comparison, because the solubility of silicon in the ferrite phase increased with increasing aging temperature, the volume fraction of coarse $D0_3$ particles precipitated in the alloy aged at 650^{o}C would decrease, as shown in Figure 5(c). This resulted that the remaining ferrite matrix would contain more silicon than that at 550^{o}C. The STEM-EDS examinations also confirm the inference, as shown in Table I. Since it is well-known that a small amount of silicon addition in Fe-Al binary alloys pronouncedly expands the (α +D03) phase field[15, 16]. It is thus to predict that owing to a higher silicon content the extremely fine $D0_3$ particles would be formed within the remaining ferrite matrix during quenching from 650^{o}C by a $\alpha \rightarrow D0_3$ continuous ordering transition, which is similar to that observed in the as-quenched alloy. For the same reason mentioned above, the coarse $D0_3$ particles would disappear gradually and the extremely fine $D0_3$ particles would be formed within the ferrite matrix during quenching in the alloy aged at temperatures above 650^{o}C. An example is shown in Figure 7. Additionally, the fact that the size of the $D0_3$ particles surrounding the β-Mn precipitates is larger than that away from the β-Mn precipitates could be observed in Figure 4(c) and 5(c). The chemical composition of the β-Mn precipitates listed in Table I shows that the chromium and silicon content is noticeably lower. This indicates that along with the formation of the β-Mn precipitates, the region surrounding the β-Mn precipitates would be enriched in silicon. Consequently, the enrichment in silicon results in a higher growth rate of the $D0_3$ phase contiguous to the β-Mn precipitates.

Finally, compared to our previous study in the Fe-8.2Al-29.7Mn-5.0Cr alloy, some discussion is appropriate. In our previous study[13], the as-quenched microstructure of the Fe-8.2Al-29.7Mn-5.0Cr alloy was the mixture of the continuous ferrite phase and the discrete austenite phase. But no evidence of the extremely fine $D0_3$ particles formed in the present as-quenched alloy could be observed within the ferrite phase in the as-quenched Fe-8.2Al-29.7Mn-5.0Cr alloy. Second, not only the precipitation of α-Mn could be preserved up to a higher temperature between 600 and 650^oC in the previous Fe-8.2Al-29.7Mn-5.0Cr alloy, but the amount of the α-Mn precipitates in the previous Fe-8.2Al-29.7Mn-5.0Cr alloy was obviously greater than that in the present alloy aged at 450^oC. However, besides the addition of 1.2 wt% Si, the chemical composition of the present alloy is similar to that in the previous alloy. Therefore, it is reasonable to believe that the Si addition to the Fe-Al-Mn-Cr alloys would not only enhance the formation of the extremely fine $D0_3$ particles within the ferrite phase during quenching, but inhibit the formation of the α-Mn precipitates.

4. Conclusions

In the present study, the phase transformations in the Fe-8.8Al-30Mn-5Cr-1.2Si alloy have been examined by transmission electron microscopy.

(1). In the as quenched condition, the extremely fine $D0_3$ particles were formed within the ferrite matrix in the alloy during quenching by a continuous ordering transition.

(2). The addition of 5.0wt.% Cr to the Fe-8Al-30Mn-1.2Si alloy would not only change the continuous ordering transition from $\alpha \rightarrow B2 \rightarrow D0_3$ to $\alpha \rightarrow D0_3$, but pronouncedly expand the $D0_3$ phase-field region.

(3). The coexistence of the $D0_3$ particles with coarse and extremely fine size has never been found in the Fe-Al-Mn-Cr-Si alloys before.

(4). The addition of 1.2 wt.% Si to the Fe-Al-Mn-Cr alloys would not only enhance the formation of the extremely fine $D0_3$ particles within the ferrite phase in the as-quenched alloy, but inhibit the formation of the α-Mn precipitates.

Acknowledgements

The author is pleased to acknowledge the financial support of this research by the National Science Council, Republic of China under Grout NSC91-2216-E-009-019.

References

1. R. wang, M.J. Straszheim and R. A. Rapp: Oxi. Met. , 1984, vol. 21 (1/2), pp. 71-79.
2. H. Erhart, R. wang and R. A. Rapp: Oxi. Met. , 1984, vol. 21 (1/2), pp. 81-88.
3. P.R.S Jackson and G.R Wallwork: Oxi.Met., 1984, vol. 21(3/4), pp. 135-70.
4. J.C. Garcia, N.Rosas and R.J. Rioja: Met. Prog.,Aug. 1982, pp. 47-50.
5. C.J. Altstetter, A.P Bentley, J.W Fourie and A.N Kirkbride: Mater. Sci. Eng., 1986, vol. 82, pp. 13-25.
6. R. Wang and F.H. Beck: Met. Prog., Mar. 1983, pp. 72-76.
7. D.J. Schmatz: Trans. ASM, 1960, vol.52, pp. 898-910.
8. T.F. Liu and C.M Wan: Scripta Metall., 1985, vol. 19(7), pp. 805-10.
9. T.F. Liu and C.M Wan: Scripta Metall., 1985, vol. 19(6), pp. 727-32.
10. T.F. Liu and C.M Wan: Scripta Metall., 1985, vol. 21(9), pp. 1212-18.
11. T.F. Liu and C.M Wan: Scripta Metall., 1985, vol. 23(7), pp. 1087-92.
12. T.F. Liu and C.M Wan: Scripta Metall., 1985, vol. 23(8), pp. 1243-48.
13. J. W. Lee, C. C. Wu and T. F. Liu: “Influence of Cr Alloying Element on Microstructures in Fe-Al-Mn-Cr Alloy”, submitted to Scripta Metall.
14. T. F. Liu, G. C. Ven, C. Y. Chao, Y. L. Lin and C. C. Wu: Metall. Trans. A, 1991, vol. 22A, pp1407-1415
15. T. Miyazaki, T. Kozakai and T. Tsuzuki: J. Mater. Sci. , 1986, vol. 21, pp.

2557-64.

16. H. P. Longworth and D. E. Mikkola: Mater. Sci. Eng. , 1987, vol. 96, pp. 213-29.

Table I. Chemical Compositions of the Phases
Revealed by an Energy-Dispersive Spectrometer (EDS)

		Chemical Composition (wt.%)				
Heat Treatment	**Phase**	**Fe**	**Al**	**Mn**	**Cr**	**Si**
As-Quenched	α+fine $D0_3$	54.94	8.76	29.76	4.93	1.25
550℃ Aging	Coarse $D0_3$	62.20	9.21	22.33	4.08	2.18
	Remaining α matrix	60.43	9.17	25.49	4.12	0.79
	β-Mn precipitate	47.07	7.66	38.53	5.97	0.77
650℃ Aging	Coarse $D0_3$	60.79	9.19	23.91	4.10	2.01
	α+fine $D0_3$	61.39	9.20	24.20	4.03	1.18
	β-Mn precipitate	47.39	8.03	37.96	5.81	0.81
750℃aging	α+fine $D0_3$	58.99	8.99	25.65	4.92	1.45
	β-Mn precipitate	46.42	8.51	38.91	5.18	0.98

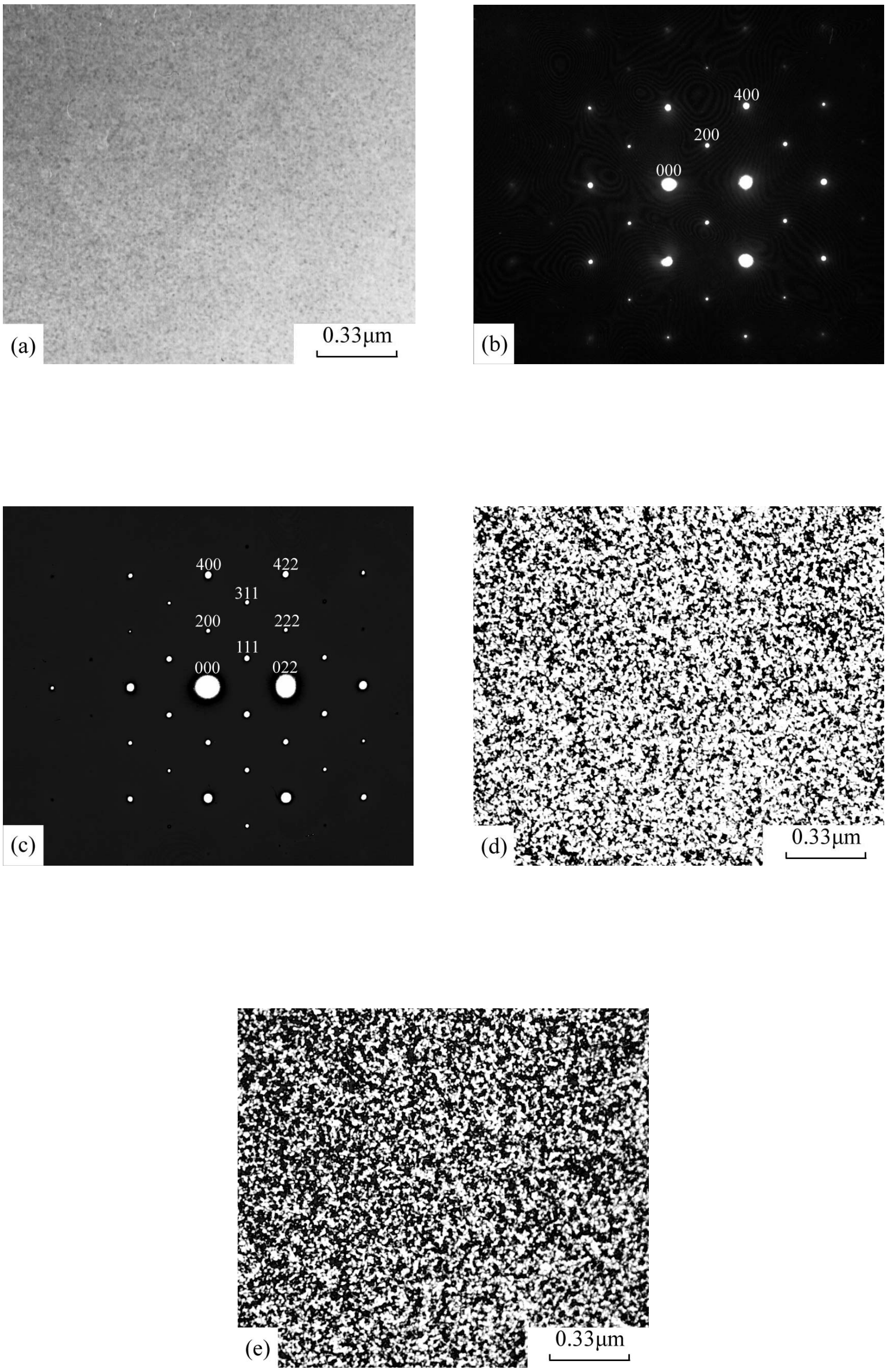

Figure 1. Electron micrographs of the as-guenched alloy, (a) BF, (b) and (c) two SADPs taken from the matrix. The zone axes are $[001]$ and $[01\bar{1}]$, respectively. (d) and (e) are 111 and 200 $D0_3$ DF, respectively.

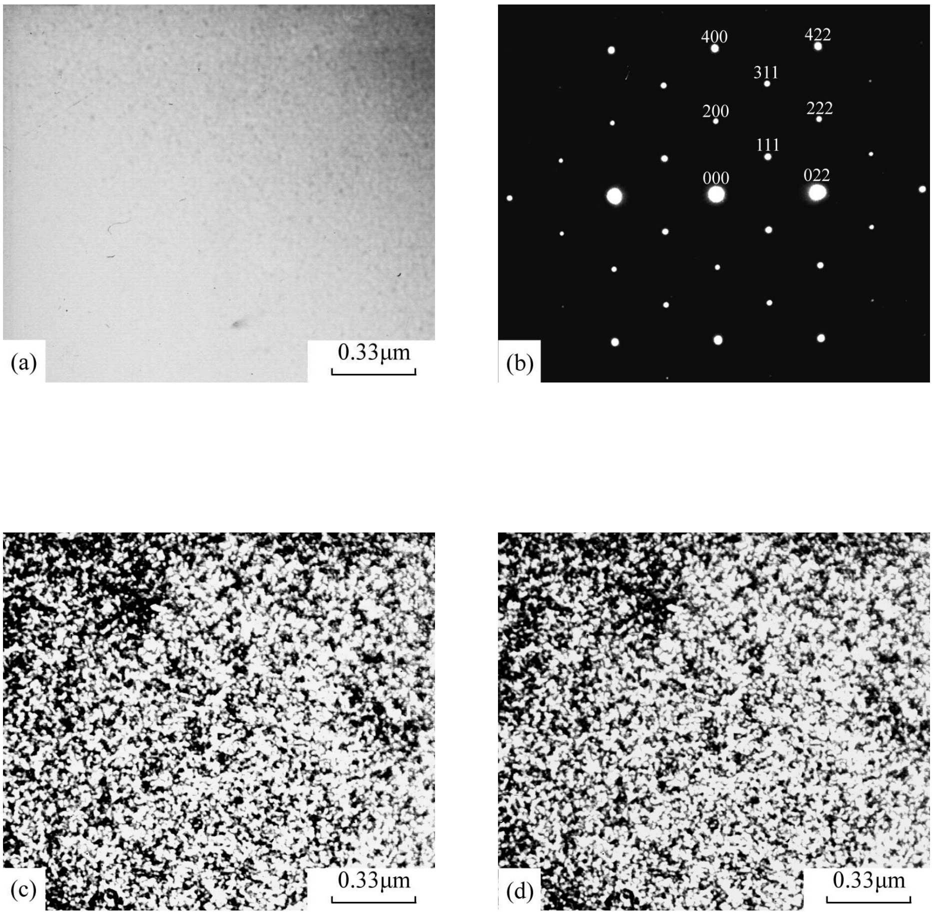

Figure 2. Electron micrographs of the alloy aged at 450℃ for 4 hours. (a) BF, (b) an SADP. The zone axis is $[01\bar{1}]$. (c) and (d) are 111 and 200 $D0_3$ DF, respectively.

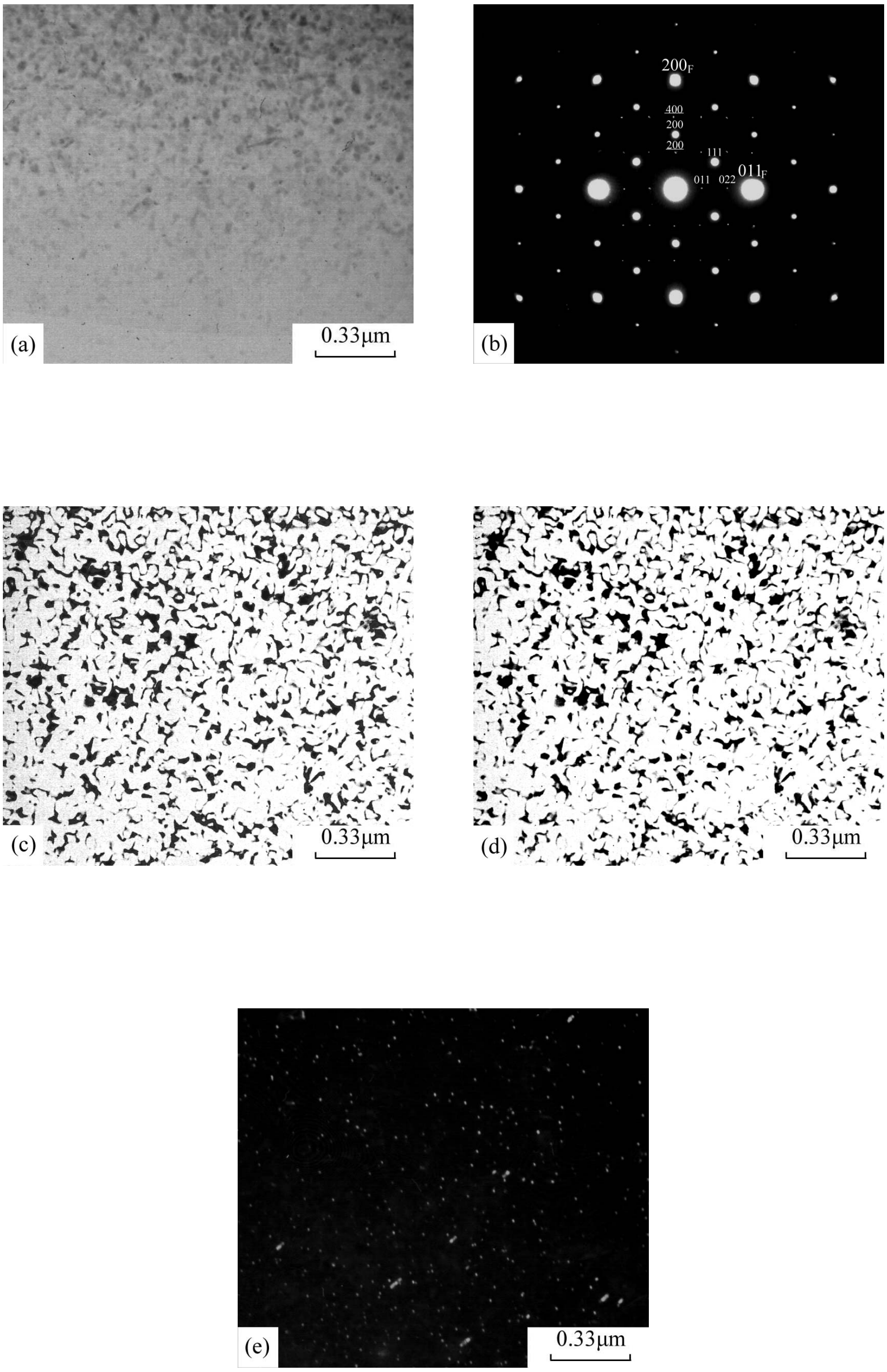

Figure 3. Electron micrographs of the alloy aged at 450℃ for 48 hours. (a) BF, (b) an SADP. The zone axis is $[01\bar{1}]$. (c) and (d) are 111 and 200 $D0_3$ DF, respectively. (e) α-Mn DF.

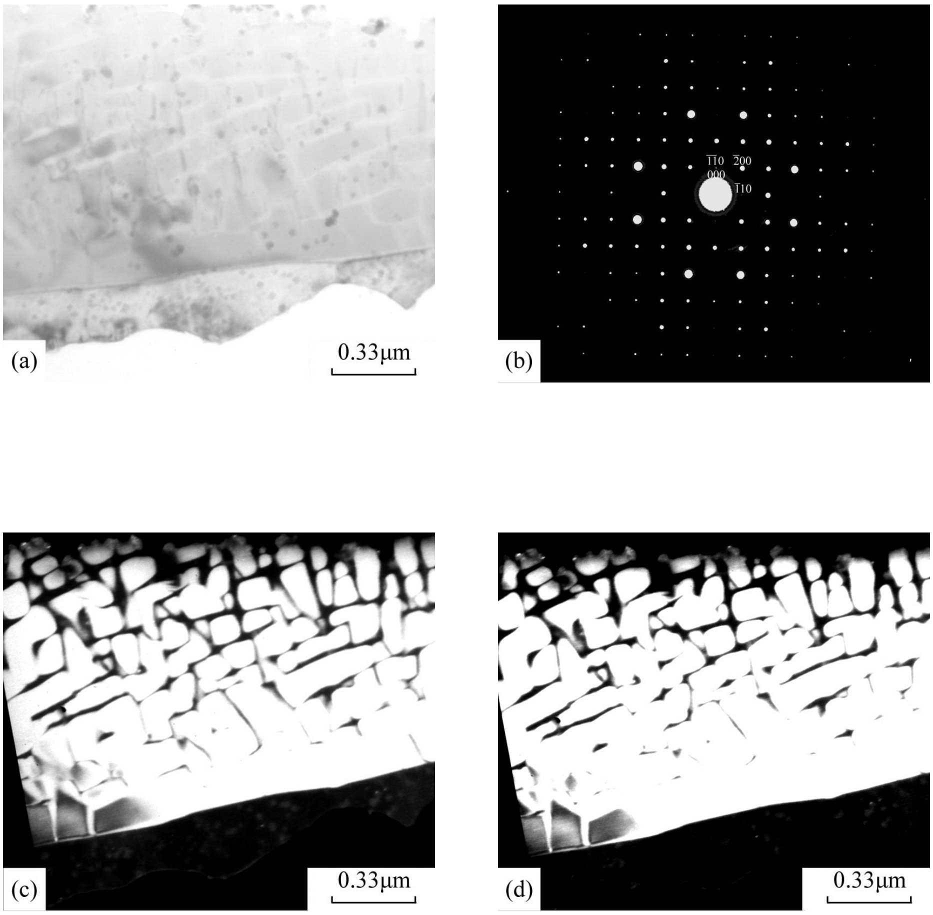

Figure 4. Electron micrographs of the alloy aged at 550℃ for 24 hours. (a) BF, (b) an SADP taken from the plate-like precipitate. The foil normal is [001]. (c) and (d) are 111 and 200 $D0_3$ DF, respectively.

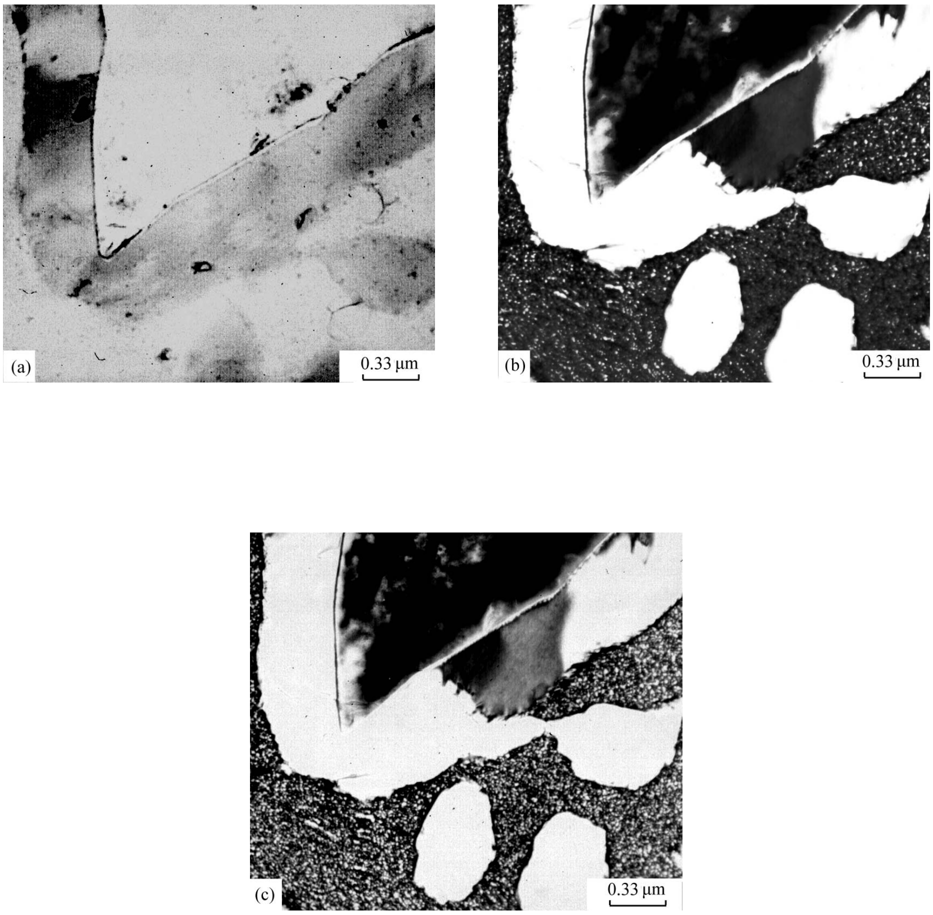

Figure 5. Electron micrographs of the alloy aged at 650℃ for 12 hours. (a) BF, (b) and (c) are 111 and 200 $D0_3$ DF.

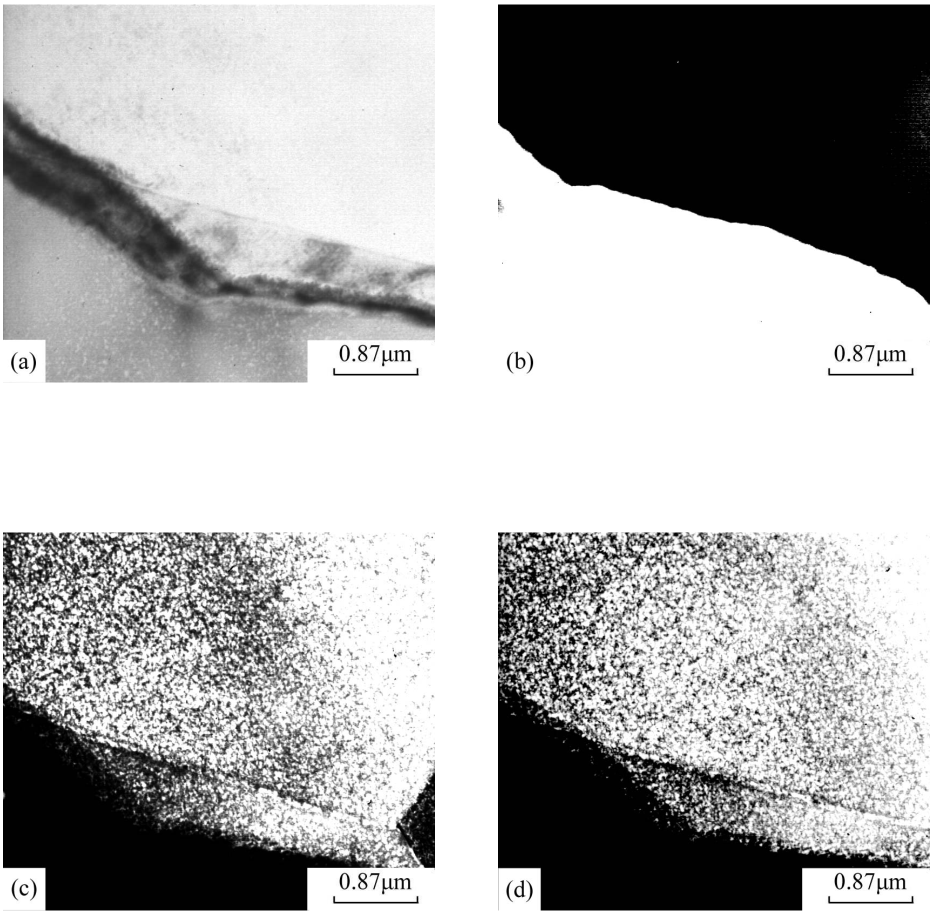

Figure 6. Electron micrographs of the alloy aged at 750℃ for 6 hours. (a) BF, (b) 110 β-Mn DF, (c) and (d) are 111 and 200 $D0_3$ DF.

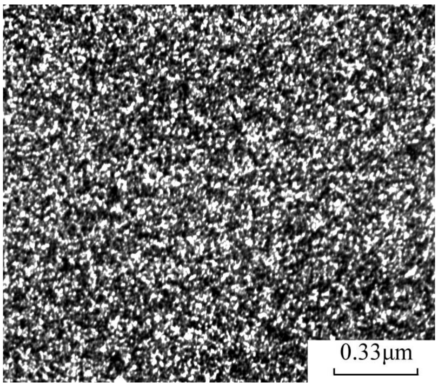

Figure 7. 111 DF electron micrographs of the alloy aged at 950℃ for 1 hour.